THE EQUIVALENCE OF SIMPLE MODELS FOR RADIATION-INDUCED IMPULSE

SAND--91-1171C

DE91 013749

R. Jeffery LAWRENCE

Computational Physics Research and Development Division
Sandia National Laboratories*, Albuquerque, NM 87185, USA

A number of models that predict the impulse generated in solid targets by short high-intensity radiation loads are described. It is shown that the impulse is insensitive to the details of the energy deposition and interaction processes. Thus with the proper nondimensionalization and normalization, all the models are shown to be very nearly equivalent.

1. INTRODUCTION

Over the past 30 years a number simple analytic models have been developed to predict the impulse generated in solid targets by short, high-intensity radiation sources. They have gone under names such as Whitener, BBAY, and Modified BBAY. Historically, they evolved in successive attempts to better match experimental observations for which the earlier versions had appeared inadequate. A good summary description of these models, including a number of variations that we will not consider here, has been given by Newlander et al.[1] We will examine just these three, but will consider two different energy deposition schemes for each. These models are all one-dimensional and share a number of common features: a threshold energy fluence; a peak impulse coupling coefficient; and at high fluences, a square-root dependence of impulse on fluence. With these similarities a reasonable question is thus: do they differ significantly? If they do, what are the differences? To answer these questions we first show in a general way that the impulse is insensitive to the details of the energy deposition and blowoff phenomena. This provides the fundamental basis for our major conclusion, which states that, with the proper choice of dimensionless variables and an appropriate normalization, all three models are essentially equivalent.

---

* Supported by the U.S. DOE under contract DE-AC04-76DP00789.

---

2. IMPULSE INSENSITIVITY

To show the sensitivity of the impulse to the specifics of the energy deposition and blowoff processes we conduct a "thought" experiment that was originally suggested by R. S. Dingus.[2] The blowoff mass that generates the recoil momentum or impulse in the target is first assumed to be broken into two arbitrary portions, as indicated in Figure 1. For a total blowoff mass of $M = m_1 + m_2$, we let

$$m_1 = f\,M \qquad \text{and} \qquad m_2 = (1 - f)\,M\ .$$

In a similar manner we let the total blowoff kinetic energy $E = e_1 + e_2$ be partitioned between the two masses according to

$$e_1 = g\,E \qquad \text{and} \qquad e_2 = (1 - g)\,E\ .$$

The respective velocities are then simply

$$v_1 = [2e_1/m_1]^{\frac{1}{2}} = [2gE/fM]^{\frac{1}{2}}\ , \qquad v_2 = [2e_2/m_2]^{\frac{1}{2}} = [2(1-g)E/(1-f)M]^{\frac{1}{2}}\ , \tag{1}$$

so that the total impulse, $I = m_1v_1 + m_2v_2$, becomes

$$I = H(f,g)\ [2ME]^{\frac{1}{2}}\ ,$$

where

$$H(f,g) = [fg]^{\frac{1}{2}} + [(1-f)(1-g)]^{\frac{1}{2}}\ .$$

Since $0 \le f,g \le 1$, the impulse function $H(f,g)$ falls within the same limits, i.e., $0 \le H(f,g) \le 1$. We also note that $[2ME]^{\frac{1}{2}}$ is the maximum possible impulse. To achieve this maximum we must have $H(f,g) = 1$, which occurs when $f = g$, and from Eq (1), leads to $v_1 = v_2$. Now by varying g we alter the manner in which the kinetic energy is partitioned between the two parts of the blowoff mass. This is analogous to a variation in the energy deposition profile. Similarly, a variation in f changes the mass distribution. In a less direct way the latter corresponds to a change in the blowoff process.

Hence, to examine the sensitivity of the impulse to changes in the energy deposition and blowoff processes we can look at the behavior of $H(f,g)$. Figure 2 is a three-dimensional plot of this impulse function where both f and g range from zero to one. As anticipated, $H(f,g)$ is a maximum, equal to one, along the diagonal. However, the more important result is that $H(f,g)$ stays relatively large except at points far out on the "wings." In fact for $0.2 \le f,g \le 0.8$ we have $H(f,g) \ge 0.8$. Similarly, even for $0.1 \le f,g \le 0.9$, $H(f,g) \ge 0.6$. Note that the heavy contours drawn on the $H(f,g)$ surface show the boundaries for these two conditions. We thus see that it takes relatively large changes in f and g to shift $H(f,g)$ appreciably from its maximum. In generalizing this, we conclude that the amount of recoil momentum generated in the target is quite insensitive to the details of either the energy deposition profile or the blowoff process.

3. SPECIFIC IMPULSE MODELS

Most investigators currently studying impulse generation from pulsed radiation loads employ one or more of the three models we will describe here. The first formulation we are considering, the Whitener model, generally gives the impulse I as

$$I = \sqrt{2} \int_0^{x_o} [\epsilon(x) - \epsilon_o]^{\frac{1}{2}} R \, dx \ , \tag{2}$$

where $\epsilon(x)$ is the energy deposition profile, and ϵ_o is a reference energy (often the vaporization energy of the target material). The material density is R, and x_o is determined from $\epsilon(x_o) = \epsilon_o$, i.e., it is the blowoff depth. The second formulation, the BBAY model, is named for its original developers, Hans Bethe, William Bade, John Averell, and Jerrold Yos. It is usually written as

$$I = \alpha \sqrt{2} \left[\int_0^{x_o} \{\epsilon(x) - \epsilon_o\} R^2 \, x \, dx \right]^{\frac{1}{2}} \ , \tag{3}$$

where $1 \le \alpha \le \sqrt{2}$, and the other parameters are as above. Finally, the modified BBAY or MBBAY model takes the form

$$I = \alpha \sqrt{2} \left[\int_0^{x_o} \{\epsilon(x) - \epsilon_o(1 + \ln \frac{\epsilon(x)}{\epsilon_o})\} R^2 \, x \, dx \right]^{\frac{1}{2}} \ , \tag{4}$$

where again $1 \le \alpha \le \sqrt{2}$. In both the BBAY and MBBAY models ϵ_o has frequently been taken as the target melt energy, although in the present study the exact definition is not important; it is simply a reference energy. The detailed derivation of these expressions is beyond the scope of this paper, however, they are described concisely by Newlander et al,[1] who also provide much of the history of their development and evolution.

To actually use these expressions we must specify the energy deposition $\epsilon(x)$. For this study we will look at two common forms, an exponential profile, and a uniform or square profile. The former is

$$\epsilon(x) = \mu \, F_o \exp[-\mu R x] \ , \tag{5}$$

where F_o is the incident fluence (energy per unit area) and μ is a mass absorption coefficient characteristic of the target material. The blowoff depth x_o follows by solving $\epsilon(x_o) = \epsilon_o$, yielding

$$x_o = \frac{1}{\mu R} \ln \frac{\epsilon_o}{\mu F_o} \ .$$

The uniform deposition profile can be written

$$\epsilon(x) = F_o/Rx_o \ , \qquad 0 \le x \le x_o \ ,$$
$$= 0 \ , \qquad x > x_o \ . \tag{6}$$

The two profiles can be related by identifying x_o in Eq (6) with the standard mean free path associated with the absorption coefficient μ, i.e., $x_o = 1/\mu R$, so that $\epsilon(x) = \mu F_o$ for $x \le x_o$. Both profiles are illustrated in Figure 3, where the shaded areas generally represent the energies available for generating impulse. With the above identification of x_o, these two energies differ only by that in the tail (beyond x_o) of the exponential profile. This will be important only at low to medium fluences, where the energy required for material vaporization is a significant portion of the total delivered energy.

We can further emphasize the similarities among the models by nondimensionalizing the principal variables, impulse I, and energy fluence F_o, as

$$I^* = \mu I/\epsilon_o^{\frac{1}{2}} \ , \qquad \text{and} \qquad F_o^* = \mu F_o/\epsilon_o \ . \tag{7}$$

Now if we assume a constant reference energy ϵ_o and a constant absorption coefficient μ, then each combination of Eqs (2), (3), and (4) with either Eq (5) or Eq (6) can be integrated to give a relatively simple expression for the impulse I^* in terms of the fluence F_o^*. The six possibilities, in dimensionless form, are summarized in Table I. To obtain specific results only the material properties R, ϵ_o, and μ are required. Note that occasional problems may require an additional integration over μ to account for a variable absorption coefficient; in principle however, a constant or "effective" value that will give reasonable results can generally be chosen.

All six of these formulations exhibit a number of features in common. Specifically, they all have the same threshold energy fluence for impulse production. As can be seen from any of the equations, it occurs when $F_o^* = 1$, or from Eq (7),

$$F_{th} = \epsilon_o/\mu \ .$$

Additionally, we can show that all of these formulations exhibit peak impulse coupling coefficients, defined as $(I^*/F_o^*)_{max}$, occurring at intermediate fluences ranging from 2 to 3 F_{th} for the uniform deposition models to 6 to 10 F_{th} for the exponential cases. Finally, for all models, the high-fluence impulse scaling can be represented by

$$I^* \sim (F_o^*)^{\frac{1}{2}} \ , \qquad F_o^* >> 1 \ .$$

4. MODEL COMPARISONS

By choosing the conventionally accepted value, $\alpha = 1.2$, in the BBAY and MBBAY models, all six expressions in Table I can be plotted, as has been done in Figure 4. Two of the features mentioned above are clearly evident. In particular, all the curves exhibit the same threshold fluence, $F_o^* = 1$, or equivalently, $F_{th} = \epsilon_o/\mu$. Since the curves are plotted logarithmically, it is easy to see that for high fluences, the impulses scale with the square root of the fluence. Once this asymptotic behavior is achieved, the various impulses differ by at most a constant. This suggests that we could bring the models into even better agreement by renormalizing the expressions given in the table. To accomplish this we simply adjust the leading constants in all six equations to yield the same asymptotic values for impulse. Alterations of this sort are reasonable because two of the three models, the BBAY and MBBAY, already contain α, which is itself somewhat arbitrary.

The results of this "equivalent normalization" are shown in Figure 5. As expected, all of the curves coalesce as the fluence becomes large. We see that the Whitener and BBAY uniform deposition models collapse onto a single curve, and, along with the MBBAY uniform deposition case, group together at the highest level of impulse. Similarly, the three exponential deposition cases group very closely together at a somewhat lower impulse level. The fact that the three exponential cases are all lower than the the others is easily explained by noting from Figure 3 that the former loose a portion of the incident energy to deposition beyond the blowoff depth. This is not true for the uniform deposition cases. This extra loss mechanism reduces the impulse, but is important mainly at low and intermediate fluences, where the amount of energy consumed in material decomposition is a major part of the incident energy. At high fluences the form of the deposition profile is clearly unimportant.

The basic conclusion that we draw from this figure is that with a specific class of energy deposition profile, the three impulse models give results that are very nearly the same. The small differences that do exist are likely to be smaller than the scatter in typical sets of experimental measurements. Thus experiments are probably not going to be able to suggest which of the models most closely predicts the real situation. Hence, we conclude that with the proper parameter definition and with equivalent normalization, the Whitener, BBAY, and MBBAY models all give results that are, in all practical situations, equivalent.

5. CLOSURE

The equivalence of these formulations was not appreciated as the models were being developed because most of the data against which they were being compared were all at fluences in the vicinity of or below the knees of the impulse curves. Perceived agreement with theory was thus strongly dependent on relatively small errors in material parameters such as the reference energy ϵ_o and the absorption coefficient μ. Further, one of the parameters, ϵ_o, was interpreted differently in one of the models. Specifically, in the MBBAY model ϵ_o was generally defined as the target material melt energy, whereas in the others it was taken as the vaporization energy, typically at least a factor of five greater. These differences in the reference energy would tend to bring the MBBAY model into better alignment with the others in the low to medium fluence regime, where the former shows somewhat less curvature. In addition, most of these early comparisons with experiment were based on nuclear test data, where the experimental environments and conditions were subject to rather large uncertainties. With these considerations it is not surprising that the similarities among the models were not recognized.

We have shown that the recoil momentum or impulse generated by the vaporization induced by pulsed radiation loads is relatively insensitive to the details of both the energy deposition and the blowoff processes. We have also shown that the three classic descriptions of this phenomenon, the Whitener, BBAY, and MBBAY models, are for all practical purposes, equivalent. Due to the forgiving nature of these formulations and the interactions they represent, there are a number of other applications for which the same general modeling approach is appropriate. We close by citing several examples to illustrate this point.

The three models were originally developed to describe the interaction of low-energy pulsed x rays with solid targets. For this situation there are no significant loss mechanisms other than those incorporated in the deposition function $\epsilon(x)$, and the impulse is independent of the radiation pulse width. In making the logical extension of this analysis to include pulsed lasers operating at IR or UV wavelengths, we find that neither of these observations apply. Consequently, we modify the fluence by

$$F_o \Longrightarrow F_o(1 - r) \ ,$$

where r is an integrated loss due to both reflection and radiation. To include a dependence on pulse width, which is manifested as thermal diffusion, we modify the absorption coefficient to

$$\mu \Longrightarrow \frac{\mu_o}{1 + \mu_o R (\alpha\tau)^{\frac{1}{2}}} \ ,$$

where τ is the pulse width, α is the thermal diffusivity of the target, and μ_o is the true absorption coefficient. The success of these simple modifications for treating laser interactions has been demonstrated in cases where the blowoff is untamped[3] (free to expand into a vacuum), and where it is fully tamped[4] (expansion is restricted). In one final example, we have even used this modeling approach to describe the enhanced momentum transfer that occurs when hypervelocity particles impact with sufficient kinetic energy to vaporize many times their own mass of the solid target.[5] Undoubtedly the future will bring other applications for this type of modeling. Hopefully, they will be as successful as the examples given here.

REFERENCES

1. C. D. Newlander et al, Nuclear Hardness Evaluation Procedures (NHEP) Program---Phase I: Analytic Technique Survey, AFWL-TR-78-18, Air Force Weapons Laboratory, Kirtland AFB, NM (1978).

2. R. S. Dingus, Los Alamos National Laboratory, Private Communication (1983).

3. R. J. Lawrence, An Effective Properties Model for Pulsed Radiation Interactions, SAND88-0245, Sandia National Laboratories, Albuquerque, NM (1988).

4. A. V. Farnsworth and R. J. Lawrence, "Numerical and Analytical Analysis of Thin Laser-Driven Flyer Plates," These Proceedings.

5. R. J. Lawrence, "Enhanced Momentum Transfer from Hypervelocity Particle Impacts," Int. J. Impact Engng, Vol. 10, pp. 337-349 (1990).

Table I
SUMMARY OF IMPULSE MODELS

Exponential Deposition	Uniform Deposition
Whitener Model	
$I^* = 2\sqrt{2}\{(F_o^*-1)^{\frac{1}{2}} - \tan^{-1}(F_o^*-1)^{\frac{1}{2}}\}$	$I^* = \sqrt{2}(F_o^*-1)^{\frac{1}{2}}$
BBAY Model	
$I^* = \alpha\sqrt{2}\{F_o^* - [1 + \ln F_o^* + 1/2\ (\ln F_o^*)^2]\}^{\frac{1}{2}}$	$I^* = \alpha(F_o^*-1)^{\frac{1}{2}}$
MBBAY Model	
$I^* = \alpha\sqrt{2}\{F_o^* - [1 + \ln F_o^* + 1/2\ (\ln F_o^*)^2 + 1/6\ (\ln F_o^*)^3]\}^{\frac{1}{2}}$	$I^* = \alpha(F_o^* - [1 + \ln F_o^*])^{\frac{1}{2}}$

FIGURE CAPTIONS

Figure 1. Schematic for momentum partitioning.

Figure 2. Impulse function H(f,g).

Figure 3. Energy deposition functions for a) exponential, and b) uniform profiles.

Figure 4. Impulse calculations with original normalization.

Figure 5. Impulse calculations with equivalent normalization.

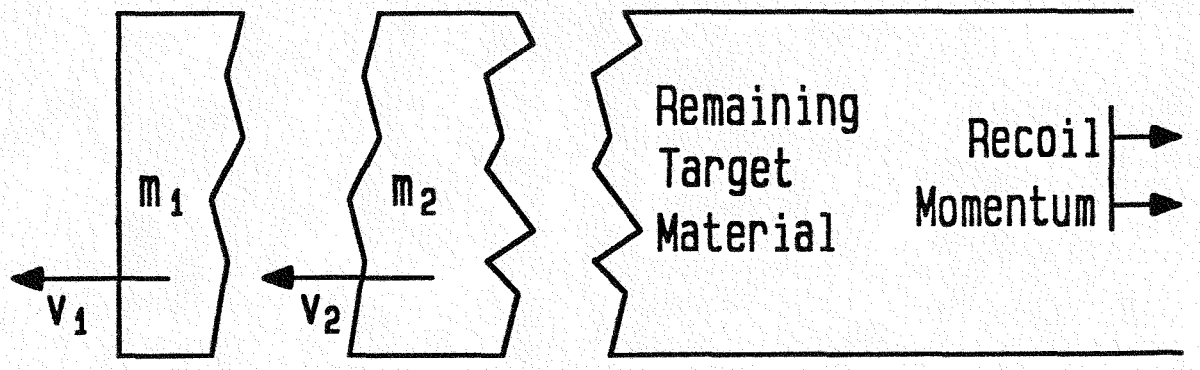

Fig. 1

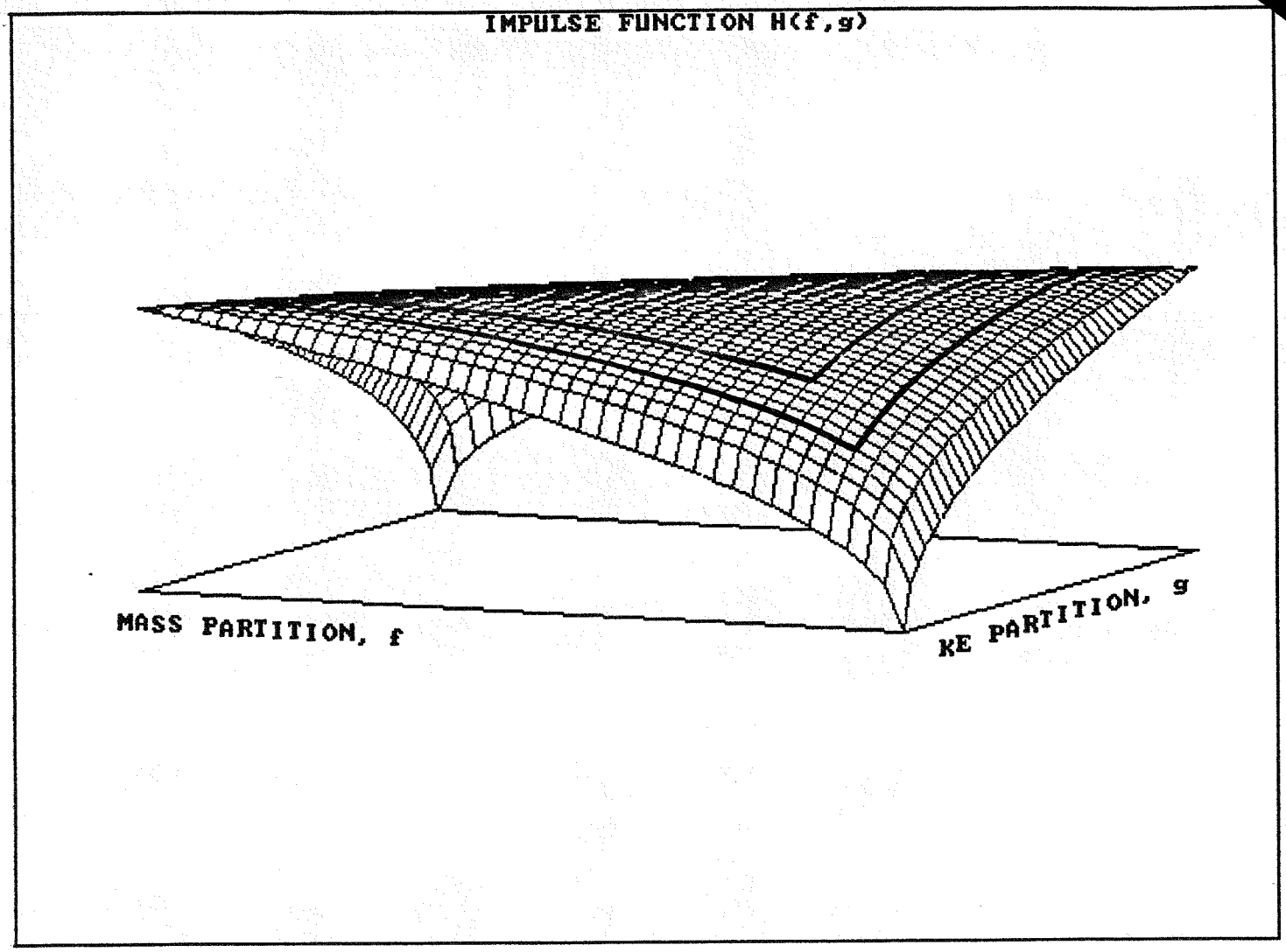

Fig. 2

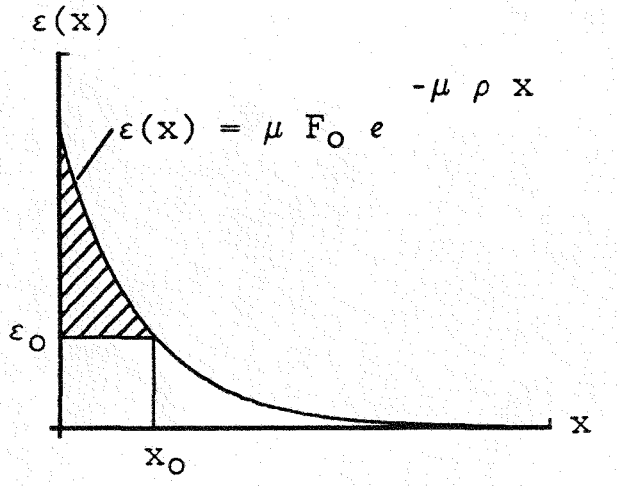

Fig. 3(a)

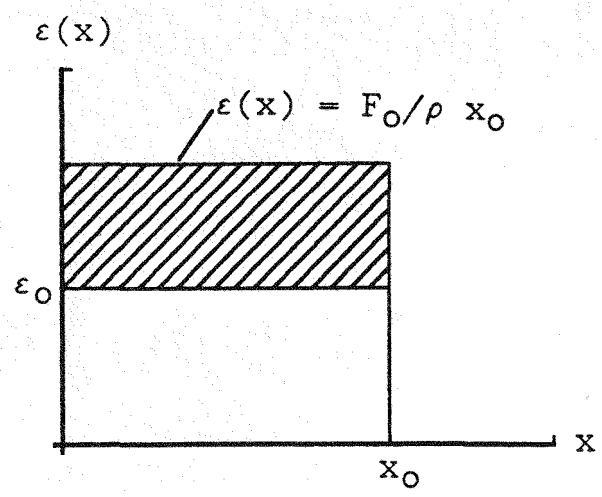

Fig. 3(b)

Text - 130%

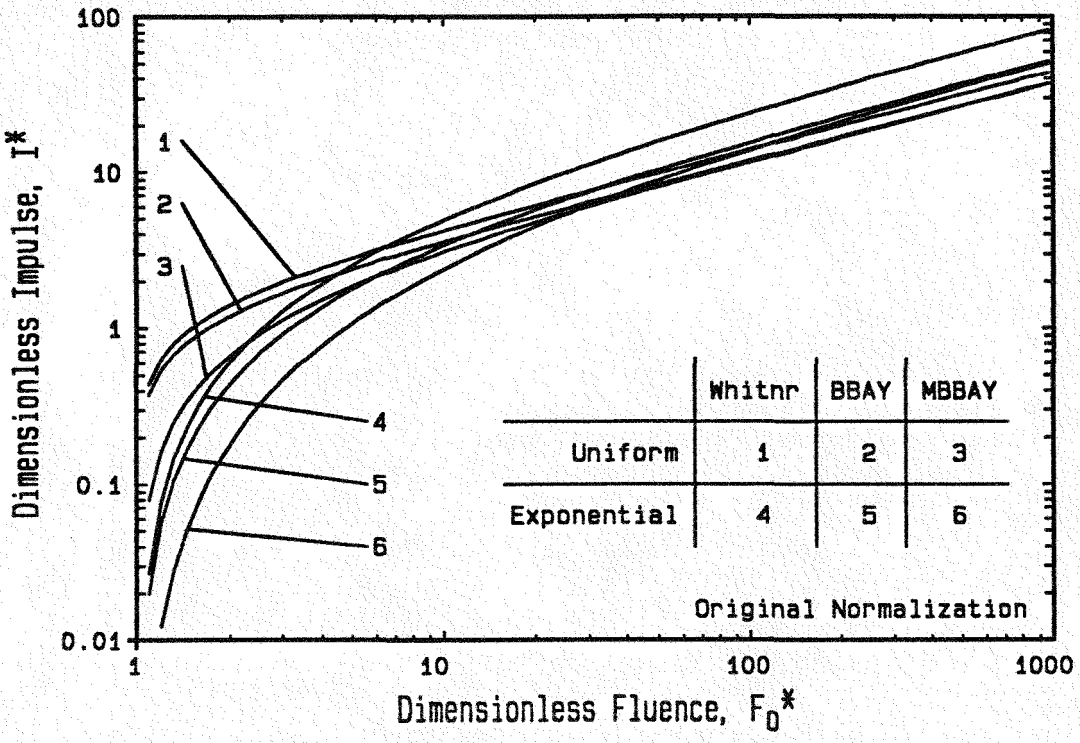
100
10
1
0.1
0.01
1
10
100
1000
Dimensionless Impulse, I*
Dimensionless Fluence, F_0*
1
2
3
4
5
6
Whitnr
BBAY
MBBAY
Uniform
1
2
3
Exponential
4
5
6
Original Normalization

Fig. A

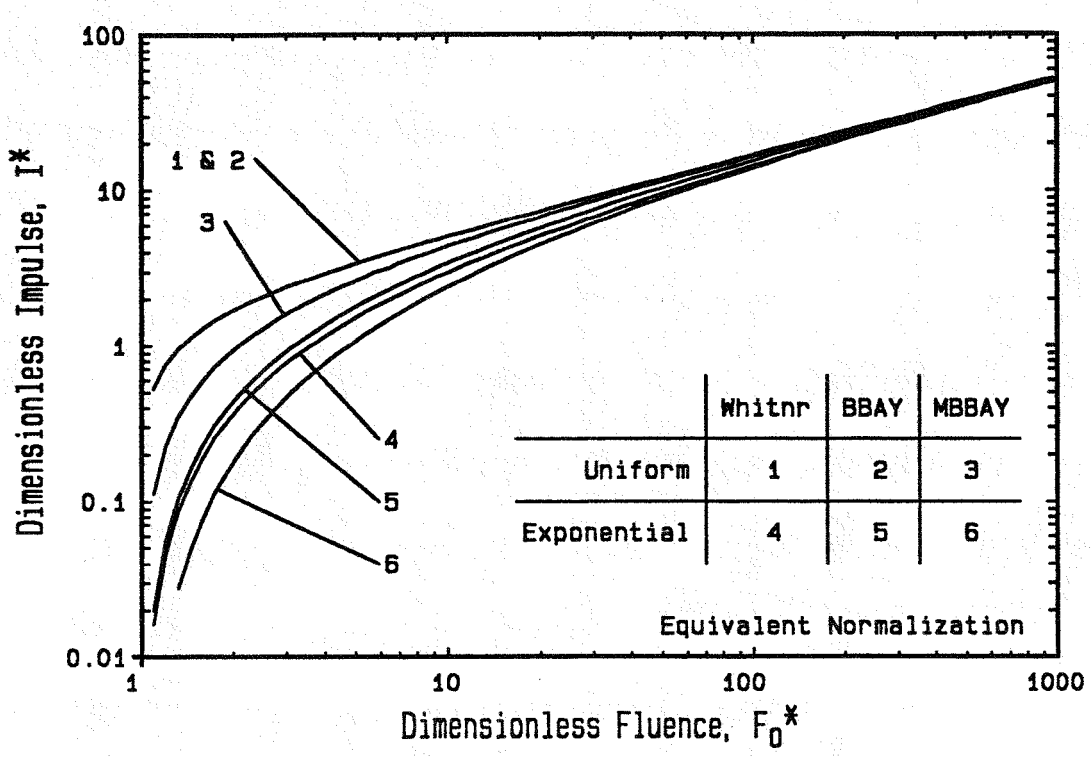
100
10
1
0.1
0.01
1
10
100
1000
Dimensionless Impulse, I*
Dimensionless Fluence, F_0*
1 & 2
3
4
5
6
Whitnr
BBAY
MBBAY
Uniform
1
2
3
Exponential
4
5
6
Equivalent Normalization

Fig. 5